We are IntechOpen,
the world's leading publisher of Open Access books
Built by scientists, for scientists

6,900
Open access books available

185,000
International authors and editors

200M
Downloads

154
Countries delivered to

Our authors are among the

TOP 1%
most cited scientists

12.2%
Contributors from top 500 universities

CLARIVATE ANALYTICS
BOOK CITATION INDEX
INDEXED

WEB OF SCIENCE™

Selection of our books indexed in the Book Citation Index
in Web of Science™ Core Collection (BKCI)

Interested in publishing with us?
Contact book.department@intechopen.com

Numbers displayed above are based on latest data collected.
For more information visit www.intechopen.com

Image Restoration Using Two-Dimensional Variations

Olga Milukova[1], Vitaly Kober[1,2] and Victor Karnaukhov[1]
[1]Institute for Information Transmission Problems of RAS,
[2]Computer Science Department, CICESE,
[1]Russia
[2]Mexico

1. Introduction

In many applications (consumer and commercial imaging, medical imaging, robotics, space research, and etc.) observed images are often degraded due to atmospheric turbulence, relative motion between a scene and a camera, nonuniform illumination, wrong focus, etc. Image restoration refers to the problem of estimating the ideal image from its observed degraded one. Numerous restoration techniques (linear, nonlinear, deterministic, stochastic, etc.) optimized with respect to different were introduced (Banham & Katsaggelos, 1997 ; Jain, 1989; Sezan & Tekalp, 1990; Bovik, 2005; Gonzalez & Woods 2008). The amount of *a priori* information about degradation such as the size and shape of blurs, noise level determines how mathematically ill-posed the problem is. *A priori* information can be used in a variety of ways in modeling and algorithm development. The information about the nature of blur (e.g., linear or nonlinear and space-variant or space-invariant) and noise (additive or multiplicative) is used in modeling the input-output relation of imaging systems. In blur modeling, when the type of blur is known (e.g., out of focus, motion, turbulence), the blurring operator can be parameterized using only a few parameters. In image modeling, the ideal image can be modeled, for instance, on the basis of *a priori* Markovian assumption. In algorithm development, *a priori* information is used in defining constraints on the solution and in defining a criterion or a quantitative description of the solution. The blind and non-blind deconvolutions were extensively studied, and many techniques were proposed for their solution (Kundur & Hatzinakos, 1996; Bertero & Boccacci, 1998; Biemond et al., 1990; Sroubek & Flusser, 2003). They usually involve some regularization which assures various statistical properties of the image or constrains on the estimated image and restoration filter according to some assumptions. This regularization is required to guarantee a unique solution and stability against noise and some model discrepancies. One of the most popular fundamental techniques is a linear minimum mean square error method. It finds the linear estimate of the ideal image for which the mean square error between the estimate and the ideal image is minimal. This linear operator acting on the observed image to determine the estimate on the base of *a priori* second-order statistical information about the image and noise processes. For images with sharp changes of intensity, the appropriate regularization is based on variational integrals (Rudin, et al.,

1992; Perona & Malik, 1990; Chan & Wong, 1998). Minimization of the variational integrals preserves edges and fine details in the image. It is obvious that quality of the restored image depends on accuracy of mathematical model of image formation process. In particular, a good estimation of distortion parameters such as speed of camera movement, transparency of atmosphere or water, etc. is very important for restoration (Biemond et al., 1990).

Recently, restoration methods based on image variations were proposed (Milukova et al., 2010a, 2010b, 2011). In this chapter, image restoration with two-dimensional variations is presented. The restored image minimizes two-dimensional variations defined by Kronrod (Kronrod, 1950). We also consider the identification of distortion operator and estimation of its parameters. It is assumed that a monochrome stationary image distorted by homogeneous integrated transformation. Various physical problems can be modeled by such transformation. The spectral method of identification of distortion parameters uses only degraded image. Computer simulation results illustrate the performance of the proposed method for restoration of blurred images.

2. Restoration of linear degraded images with variation methods

2.1 Variation concept for image restoration

Image restoration problem is usually formulated as follows. Undistorted (original) image z is recovered from the given equation:

$$v = Az + n \ , \tag{1}$$

where $A : Z \to Q$ (Z, Q are metric spaces) is linear or nonlinear operator, $z \in Z$, n is noise, v is observed distorted image. A general approach for image restoration can be formulated using statistical estimation methods and the theory of solving of ill-posed problems (Tikhonov & Arsenin, 1977). The restoration problem is a typical inverse problem of mathematical physics, and, therefore, it can be correctly solved on the base of mathematical methods. The restored image can be obtained by minimization of the following functional:

$$z^* = \inf_{z \in Z} \rho_Q(Az, v) \ , \tag{2}$$

where ρ_Q is a metric in Q. Note that various definitions of a distance ρ_Q between two images may be used. It is easy to show that the solution of the optimization problem in Eq. (2) is not unique even when the operator A and the distorted image v are exactly known, and no additive noise. *A priori* information about the original image should be used to obtain a unique and stable solution from the set of solutions. The simplest way to guarantee uniqueness and stability of the solution is to describe the image model with a functional $\Omega(z)$ that possesses stabilizing properties. In this case the image restoration problem can be reduced to conditional or unconditional optimization problem, in particular to the Tikhonov's minimization (Tikhonov & Arsenin, 1977),

$$z^* = \inf_{z \in Z} \{ \rho_Q(Az, v) + \alpha \Omega(z) \} \ , \tag{3}$$

where α is a parameter of regularization. Note that the statistical methods used in image restoration lead to optimization problems, which are similar to that of Eq. (3). For instance, using Bayes' strategy (Kay, 1993) we can obtain the optimal estimation in the following form:

$$z^* = \inf_{z \in Z} \{-\ln p_2(Az - v) - \ln p_1(z)\} \,, \tag{4}$$

where $p_1(\xi)$ and $p_2(\xi)$ are *a priori* probability densities of the original image z and additive noise $n = Az - v$. The main difference between the regularization method of image restoration in Eq. (3) and the statistical method in Eq. (4) is the regularization parameter α. This leads to a family of solutions as a function of the parameter α. The best restored image can be chosen from the set of solutions using, for instance, a subjective criterion. If the space Q in Eq. (3) is the Euclidian space with the norm (v, Bv), where B is a positive defined operator, we obtain,

$$z^* = \inf_{z \in Z} \{\|Az - v\|_B^2 + \alpha \Omega(z)\} \,. \tag{5}$$

It is commonly assumed that the original image is a smooth function with respect to the Sobolev space (Adams, 1975), and the stabilization functional in Eq. (5) is $\Omega(z) = \|z\|_{W_q^p}^q$. Quadratic forms can be used in order to avoid nonlinear restoration algorithms. Note that a Gaussian image model leads to minimization of a quadratic form. In discrete case it corresponds to the Sobolev norm for $p = 2$ in Eq. (5). On the other hand, the use of quadratic forms in image restoration often yields undesirable results because of real images are not Gaussian. Now suppose that an image to be restored is a function of bounded variations. Therefore, it may be written as

$$z^* = \inf_{z \in Z} \{\rho_Q(Az, v) + \alpha Var(z)\} \,. \tag{6}$$

The variation of a 1D function $f(x)$, $x \in [a, b]$ is defined as follows:

$$\overset{b}{\underset{a}{V}}(f) = \sup_{x_1 \dots x_n} \sum_{k=2}^{n} |f(x_k) - f(x_{k-1})| \,. \tag{7}$$

It can be shown, that if the image $z(x, y)$, $(x, y) \in D$ consists of 1D functions of bounded variation along its rows and columns then the image is also a 2D function of bounded variation. Different multidimensional variations were proposed such as variations of Arzela, Vitali, Tonelly, etc. (Vitushkin, 1955). A different approach was suggested by Kronrod, who introduced two functionals in order to describe an image as a function of two variables (Kronrod, 1950). The functionals are given as follows:

$$d_1(z) = \int_{-\infty}^{\infty} m_0(e_t) dt \,, \text{ and } d_2(z) = \int_{-\infty}^{\infty} m_1(e_t) dt \,, \tag{8}$$

where e_t is t - level set of the function $z(x, y)$, i.e. a set of points (x, y) with function values equal to t, $m_0(e_t)$ is the number of components of e_t, and $m_1(e_t)$ is the length of the set e_t.

The class of functions of bounded variations given in Eq. (8) is very extensive. These functions possess the following attractive properties: they are differentiable almost everywhere and their Fourier series are convergent almost everywhere. Note that numerous attempts to create a mathematical image model with the help of one functional were unsatisfactory. It can be done on the base of two (independent in a certain way) functionals. It is interesting to point out, that the first variation d_1 in Eq. (8) is a topological characteristic of the image. If the original image is a continuous differentiable function, then the second variation can be represented as

$$d_2(z) = \int\limits_a^b \int\limits_c^g |grad\, z(x,y)|\, dx\, dy\,. \tag{9}$$

If only the second variation is used, the image restoration can be carried out as follows (Perona & Malik,1990):

$$z^* = \inf_{z \in Z} \{ |Az - v|_B^2 + \alpha \int\limits_a^b \int\limits_c^g |grad(z(x,y))|\, dx\, dy \}\,, \tag{10}$$

where *grad(.)* is a gradient operator.

It is of interest to note that this nonlinear method of image restoration minimizes the functional that is identical to the Kronrod's second variation. We propose to minimize the functional in Eq. (10) subject to constraint on the first Kronrod's variation of the image. This approach is referred to as conditional variation approach (Milukova et al., 2010). Next with the help of computer simulation we illustrate the difference in the performance of two variation methods: minimization of the functional in Eq. (10) and conditional minimization of the same functional. Additionally, the performance of minimum norm image restoration from Eq. (10) without considering variations is also provided.

2.2 Restoration of uniformly blurred image with spatial variations

The impulse response of the 1D uniform blur can be expressed as follows:

$$h_L(x) = \begin{cases} 1/L, & \text{if } 0 \le x \le L-1 \\ 0, & \text{otherwise} \end{cases}\,, \tag{11}$$

where *L* determines a blur extension. It is known that point spread functions for such blurs do have zeros in the frequency domain, and they can be uniquely identified by the location of these zero crossings (Cannon, 1976; Gennery, 1973). If the original image is blurred and noiseless then the blur matrix *A* in Eq. (1) is given as

$$A = 1/L \left\|
\begin{array}{cccccc}
1 & 1 & \dots & 1 & & \\
 & 1 & 1 & \dots & 1 & D_2 \\
 & & 1 & 1 & \dots & 1 \\
 & & & 1 & 1 & \dots & 1 \\
D_1 & & . & . & . & . & . \\
 & & & 1 & 1 & \dots & 1
\end{array}
\right\|_{MxN}\,, \tag{12}$$

and the linear system of equations in Eq. (1) is rewritten as

$$Az = D_1 z_L + D_2 z_R = v , \qquad (13)$$

where $z_L = \{z_1, ..., z_{L-1}\}$, $z_R = \{z_L, ..., z_N\}$, $M=N-L+1$. A general solution of Eq. (13) can be written as

$$z^* = z^p + \sum_{m=1}^{B} \beta_m \mathbf{e}_m , \qquad (14)$$

where $\mathbf{e}_m$ is a basis of kernel A, $\{\beta_m\}$ are real variables, $z^p = \{z_L, D_2^{-1}(v - D_1 z_L)\}$ is a particular solution of linear system of equations in Eq. (13). Suppose that $z_L = 0$, the particular solution can be expressed as

$$z^p = \{0, D_2^{-1} v\} . \qquad (15)$$

The basis $\mathbf{e}_m$ can be found from Eq. (13) as

$$\mathbf{e}_m = \{e_L^m, -D_2^{-1} D_1 e_L^m\} , \qquad (16)$$

where $e_L^m = \{\delta_{1m}, \delta_{2m}, ..., \delta_{L-1m}\}$, δ_{ij} is the Kronecker delta function. The basis of kernel A has the following form:

$$\begin{Vmatrix} 1 & & -11 & & -1 & 1 & & -1 \\ & 1 & & -1 & 1 & & -1 & & 1 & & -1 \\ & & & & & .... & & & \\ . & . & . & . & & & . & . \\ & & 1-1 & & & 1-1 & & & 1-1 \end{Vmatrix} .$$

It is of interest to note that the basis of kernel A contains vertical columns of unities; therefore, a general solution of Eq. (13) could contain a periodic structure with the period of blurring (Buades et al., 2006). In our computer simulation we compared three methods: 1) first, substituting Eq. (15) into Eq. (10) and minimizing the functional with respect to $\{\beta_m\}$; 2) the second method minimizes the same functional subject to the first Kronrod's variation given in Eq. (8), which is taken close to that of the original image; 3) minimum norm image restoration from Eq. (10) without considering variations. Actually, if the inverse of the blur operator exists, it can be applied to the observed image to obtain an estimate. This is called inverse filtering. The estimate differs from the actual image by the additional error of amplified noise, and depending on the nature of the blur operator and the noise, it may drastically obscure the desired image information. Hence, inverse filtering is extremely noise sensitive. If the inverse operator does not exist, a solution can be found on the basis of a least squares criterion. A least squares solution minimizes the norm of the residual signal Az-v. The least squares solution with minimum norm (energy) is called also the pseudoinverse filtering (Jain, 1989). The first tested method is referred to as Grad method, the second one is called Grad-conditional method, and the last method is named Min-norm method. Fig. 1(a) shows a test input image used in experiments. The size of the image is

256×256 pixels, $N=256$. The signal range is [0-255]. The test input scene is homogeneously blurred with $L=7$. The blurred image is shown in Fig. 1(b).

(a)

(b)

Fig. 1. (a) Test image, (b) test image uniformly blurred in horizontal direction with L=7.

The original image has the following values of the Kronrod variations: $d_1=2105$, $d_2=12210$. The results of image restoration with the variation methods are shown in Figs. 2(a) and 2(b), respectively. The restoration result with the Min-norm algorithm is shown in Fig. 2(c). Subjective visual criterion is defined as an enhanced difference between original and restored images. A pixel is displayed as gray if there is no error between the original image and the restored image. For maximum error, the pixel is displayed either black or white (with intensity values of 0 and 255, respectively).

(a)

(b)

(c)
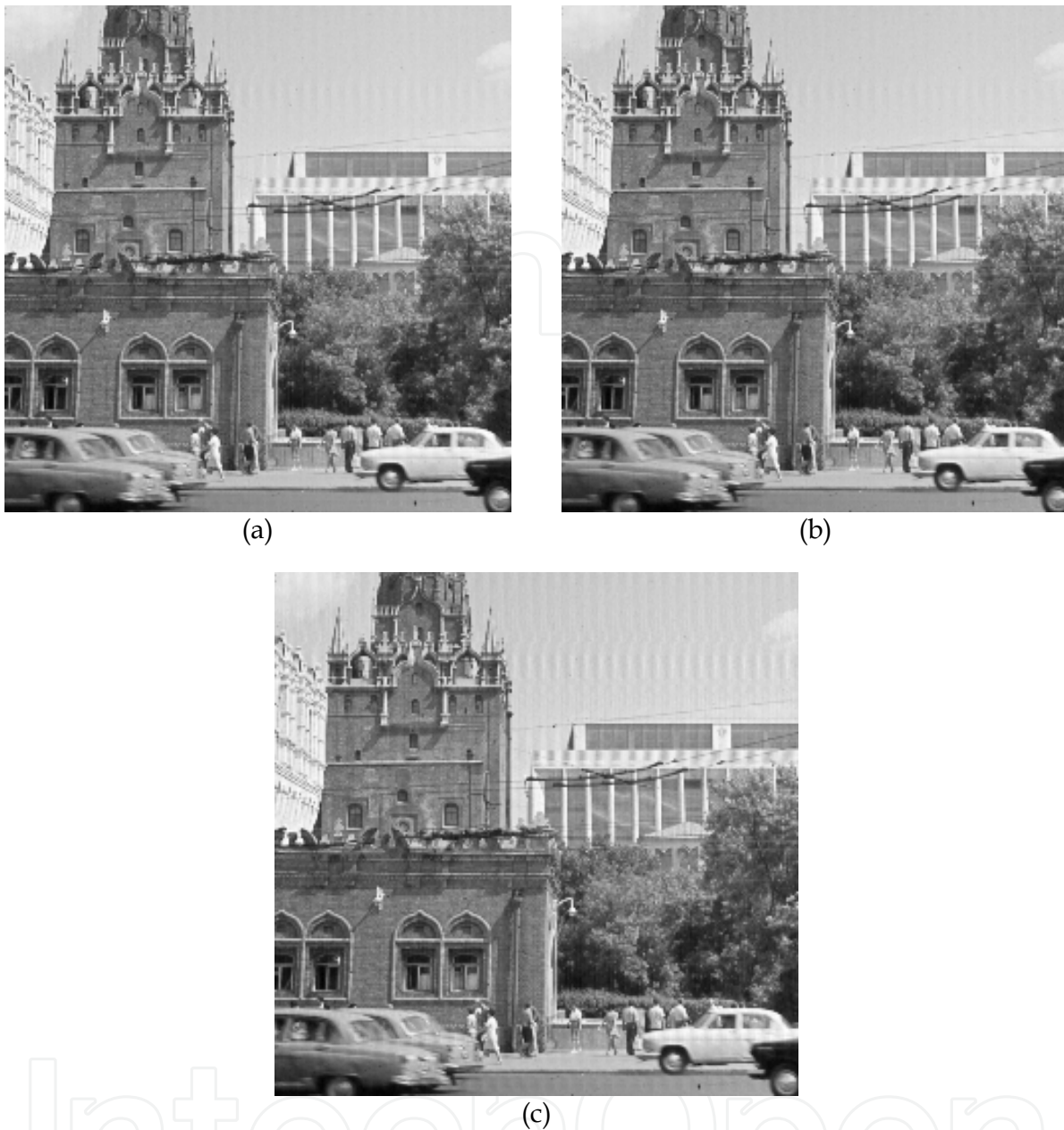
Fig. 2. Image restoration with (a) Grad method, (b) Grad-conditional method, and (c) Min-norm method.

Figs. 3(a), 3(b), and 3(c) show differences between the original image and that of restored with the Grad algorithm, the Grad-conditional algorithm, and the Min-norm algorithm, respectively. We see that the second algorithm, which takes into account two Kronrod's variations yields the best recognition performance. A quantitative comparison is given by the peak signal-to-noise ratio (PSNR),

$$PSNR(z, z^*) = 20\log_{10}\left(\frac{255}{\|z - z^*\|}\right).\tag{17}$$

(a)

(b)

(c)
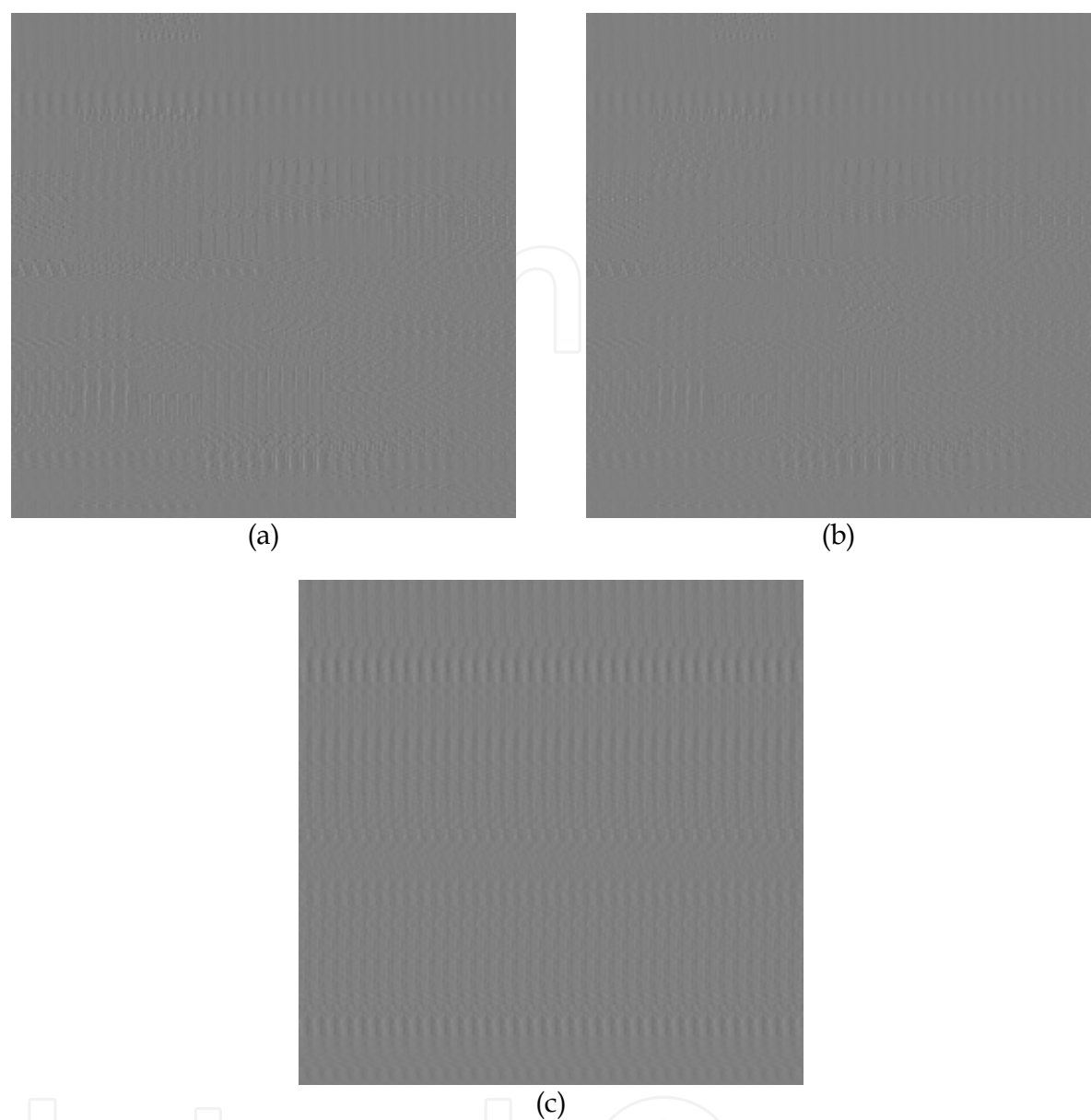
Fig. 3. Differences between the original image and restored with (a) Grad method, (b) Grad-conditional method, and (c) Min-norm method.

The image restored with the Grad method has d1=2050, d2=12015, the image restored with Grad-conditional method has d1=2103, d2=12120, and finally, the image restored by the Min-norm method possesses d1=2218, d2=12343. Table 1 shows the restoration performance of the tested methods in terms of the PSNR versus the blur extension.

L	Min-norm	Grad	Grad-conditional
3	28.3	34.5	35.2
5	25.1	30.2	31.3
7	22.2	28.5	29.4
9	18.4	26.2	27.3

Table 1. PSNR (dB) results for the tested methods.

So, in order to achieve a good restoration, it is important take into account topological characteristics of the image to be restored. These characteristics can be described by the first Kronrod's variation.

3. Identification of degradation operators and estimation parameters in the Fourier domain

In this section, identification of operator degradation type and estimation of distortion parameters is discussed. Monochrome stationary image distorted by homogeneous linear transformation is considered. Various physical problems can be modeled by such degradations (Bertero & Boccacci, 1998). Identification of the distortion operator is carried out using the Fourier spectrum of the distorted image. Automatic image restoration is performed in three steps, that is, i) identification of distortion operator, ii) estimation of distortion parameters, and iii) image restoration with estimated parameters. Certain types of distortion operators are completely characterized by attributes such as the location of frequency-domain zeros. The techniques (Cannon, 1976; Gennery, 1973) make the following two assumptions: (i) the blurring produces zero crossings in the frequency domain and it can be completely characterized by the location of these zero crossings, and (ii) the location of zero crossings can be determined from the Fourier transform or power cepstrum (the logarithm of the power spectrum) of the observed image. These methods are very simple to use and they can successfully applied in many real-life situations. It is indeed true that the models for motion and focus blurs do have zeros in the frequency domain, and they can be uniquely identified by the location of these zero crossings. On the other hand, blurring models that do not have zero crossings in the frequency domain (e.g., Gaussian modeling atmospheric turbulence) cannot be identified by these techniques. Furthermore, the identification of the zero crossings from the observed image may be quite difficult due to the presence of strong observation noise. Almost all practical implementations of the restoration algorithms assume that the observation noise is a zero-mean, white Gaussian process that is uncorrelated to the image signal. In this case, the noise field is completely characterized by its variance, which is commonly estimated by the sample variance computed over a low-contrast local region of the observed image (Yaroslavsky & Eden, 1996).

Let us consider an observed image degraded with a linear spatially invariant system and additive sensor noise, that is,

$$v = Az + n = \int\limits_{-\infty}^{\infty} \int\limits_{-\infty}^{\infty} h(x - \xi, y - \eta)z(\xi, \eta)d\xi d\eta + n(x, y), \qquad (18)$$

where $h(x, y)$ is the impulse response of the system. The Fourier spectrum of the observed image is given by

$$V(\omega_1, \omega_2) = H(\omega_1, \omega_2)Z(\omega_1, \omega_2) + N(\omega_1, \omega_2), \qquad (19)$$

where $H(\omega_1, \omega_2)$ is the frequency response of the liner degradation filter, $V(\omega_1, \omega_2)$, $Z(\omega_1, \omega_2)$, and $N(\omega_1, \omega_2)$ are spectra of the observed image, original image, and noise realization, respectively. Several typical examples of linear degradations are provided (Jain,

1989). Motion blur occurs when there is relative motion between the object and camera during exposure. In this case the impulse response and the frequency response of the linear system of horizontal motion blur are given, respectively, as

$$h(x,y) \; = \; \frac{1}{L} rect\left(\frac{x}{L} - \frac{1}{2}\right)\delta(y), \tag{20}$$

$$H(\omega_1,\omega_2) \; = \; e^{-i\pi w_1 L} \text{sinc}(w_1 L), \tag{21}$$

where L is the motion path, $rect(x) = 1$, *if* $x \in [0,1]$, *else* 0, $\delta(y)$ is the Dirac delta function.

Atmospheric turbulence is a common blur in remote sensing and aerial imaging. For long term exposure through the atmosphere Gaussian model is used. So, the impulse response and the frequency response of the linear system of turbulence blur are given, respectively, as

$$h(x,y) \; = \; e^{-\pi a^2 (x^2 + y^2)}, \tag{22}$$

$$H(\omega_1,\omega_2) \; = \; \frac{1}{a^2} e^{\frac{-\pi(\omega_1{}^2 + \omega_2{}^2)}{a^2}}, \tag{23}$$

where a is the parameter that determines the severity of blur.

Defocusing is another common type of blurring owing to the finite size of the camera aperture. When the defocusing blur is large, the following uniform model is used. The impulse response and the frequency response of the linear system can be expressed, respectively, as

$$h(x,y) \; = \; \begin{cases} \frac{1}{\pi r^2}, x^2 + y^2 \le r^2 \\ 0, \text{ elsewhere} \end{cases}, \tag{24}$$

$$H(\omega_1,\omega_2) \; = \; \frac{J_1(rp)}{rp}, \; p = \omega_1{}^2 + \omega_2{}^2, \tag{25}$$

where J_1 is the first-order Bessel function.

Image blurring also occurs in image acquisition by scanners in which the image pixels are integrated over the scanning aperture. Example of such degradations can be found in image capturing by radar, beam-forming arrays, and display systems using television raster. The impulse response and the frequency response of the linear system can be written, respectively, as

$$h(x,y) \; = \; rect\left(\frac{x}{a}, \frac{y}{b}\right), \tag{26}$$

$$H(\omega_1,\omega_2) = ab\text{sinc}(a\omega_1)\text{sinc}(b\omega_2), \tag{27}$$

where $a \times b$ is the rectangular aperture.

It is of interest to compare the spectra of the original and degraded images. From numerous experiments it is known, that the spectral magnitude of a realistic image is not very informative. It contains information about distribution of the signal energy in the frequency domain. For instance, if we exchange the spectral magnitudes of two similar images belonging to the same class and perform the inverse Fourier transform, then the difference in visual appearance of the original and obtained images will be negligible (Yaroslavsky & Eden, 1996). However, the difference between the spectral magnitudes of the original and degraded images may be significant due to the spectral magnitude of the frequency response of the linear system. Figs. 4(a) and 4(b) show a test original image and its spectral magnitude.

(a)   (b)
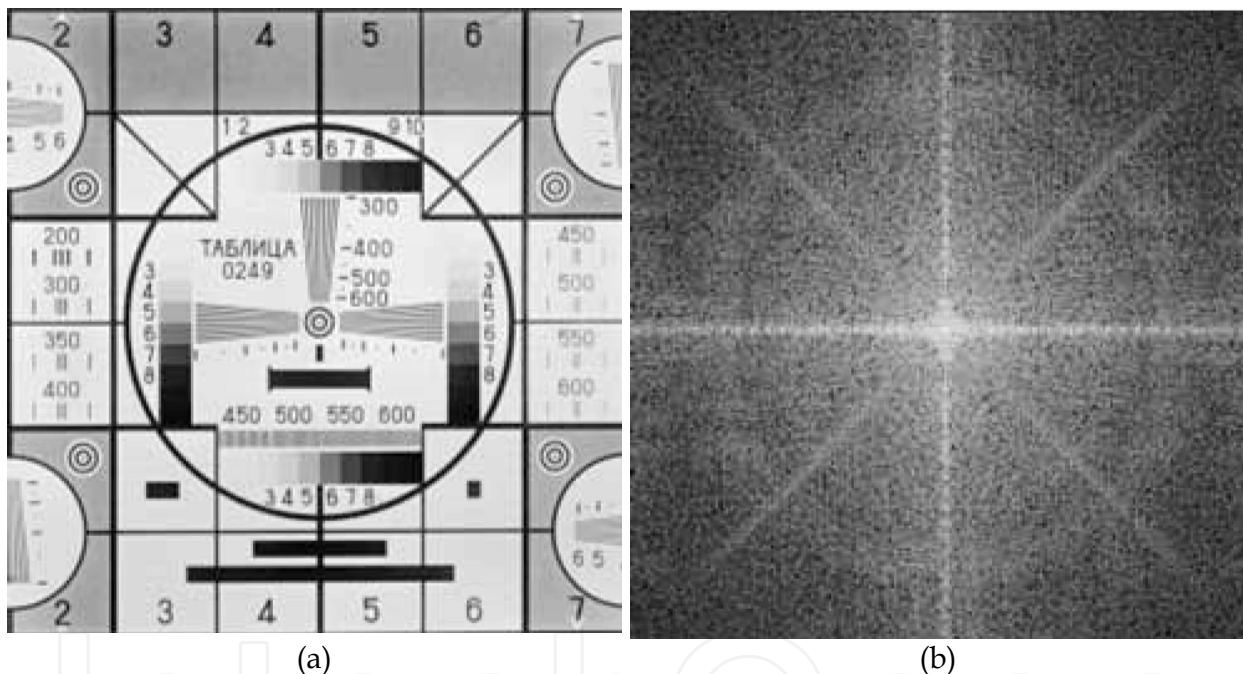
Fig. 4. (a)Test original image, (b) spectral magnitude of the original image.

In order to identify the distortion operator a database containing various images of spectral magnitudes was created. Training elements of database were obtained on the base of mathematical modeling or computer simulation. In practice, the number of degradation operators is not very large. Next, the spectral magnitude of a degraded image is matched to those of the database. This simple recognition system works well to identify the type of degradation operator for common blurs. Figs. 5 illustrate spectral magnitudes for different common blurring operators. One can observe that spectral magnitudes of distorted images contain mainly the information about distortion operators such as zero crossings on the plane (ω_1, ω_2).

(a)

(b)

(c)

(d)

(e)

(f)

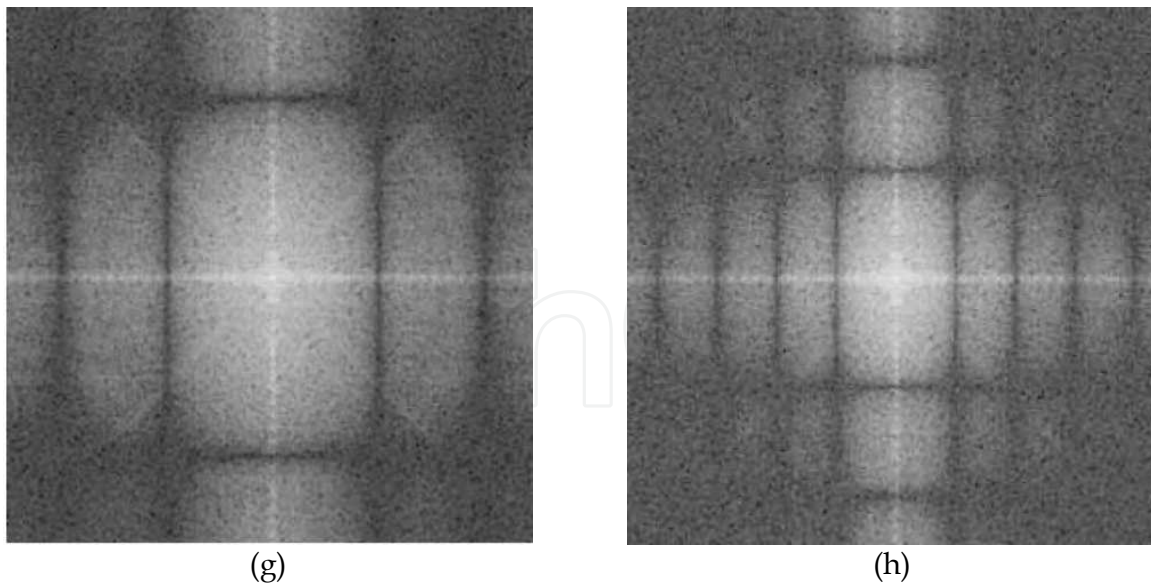(g)   (h)
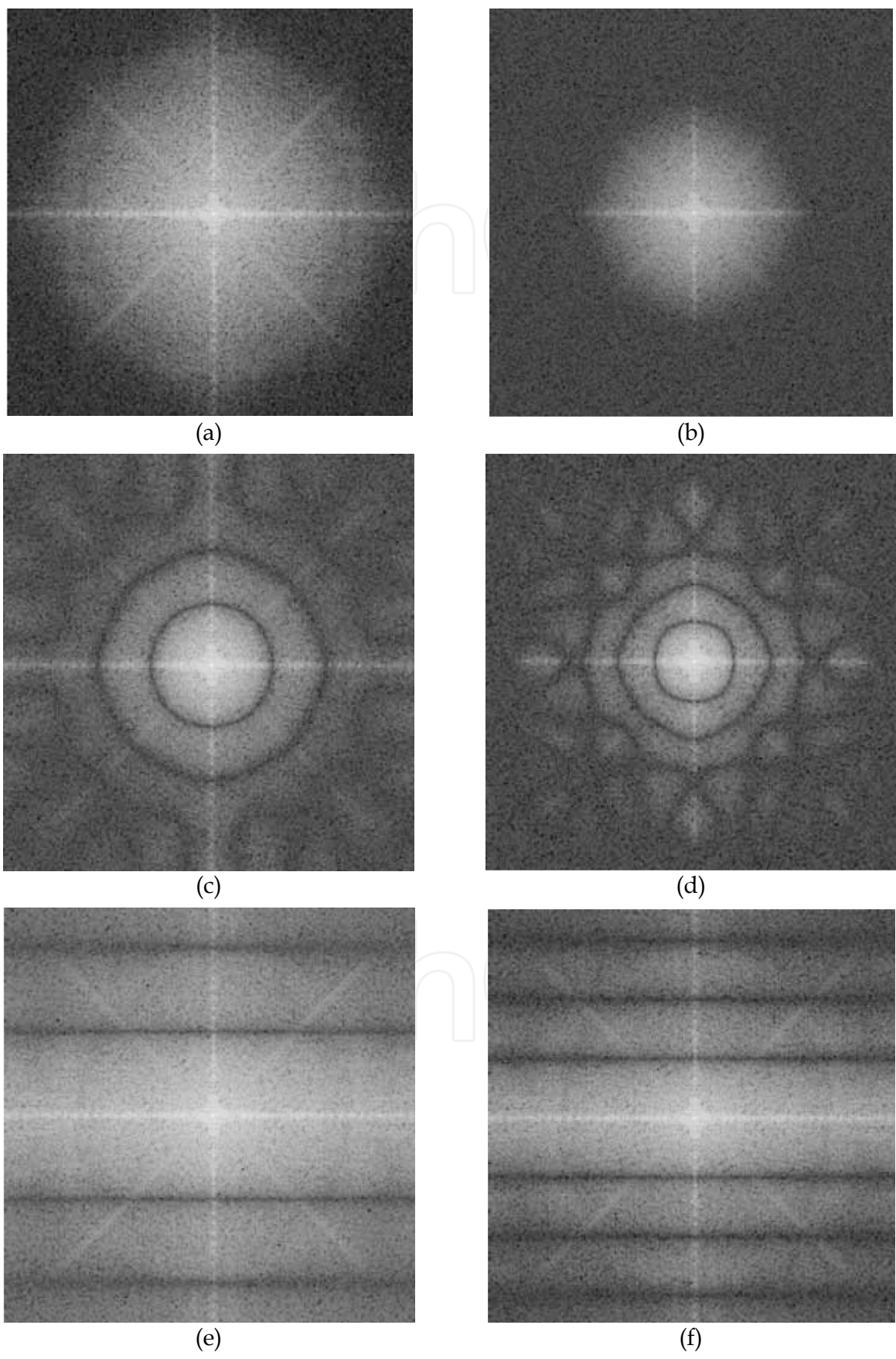
Fig. 5. Spectral magnitudes of the test original image shown in Fig. 4(a) degraded by: (a) atmosphere turbulence defocusing (Eq. 23) with $a = 2$, (b) atmosphere turbulence defocusing (Eq. (23) with $a = 4$, (c) isotropic defocusing (Eq. 25) with $r = 4$, (d) isotropic defocusing (Eq. 25) with $r = 6$, (e) 1D motion blur (Eq. 21) with $L = 4$, (f) 1D motion blur (Eq. 21) with $L = 6$, (g) convolution with rectangular aperture (Eq. 27) with $a=4$, $b=2$, and (h) convolution with rectangular aperture (Eq. 27) with $a=8$, $b=4$.

Actually, composite degradations can be considered as a combination of the basic distortion operators. In this case, the Fourier spectrum of a new composite operator is the product of the spectra of used basic operators. Figs. 6(a) and 6(b) show the spectral magnitudes of the test original image degraded with isotropic blur and horizontal motion.

(a)   (b)
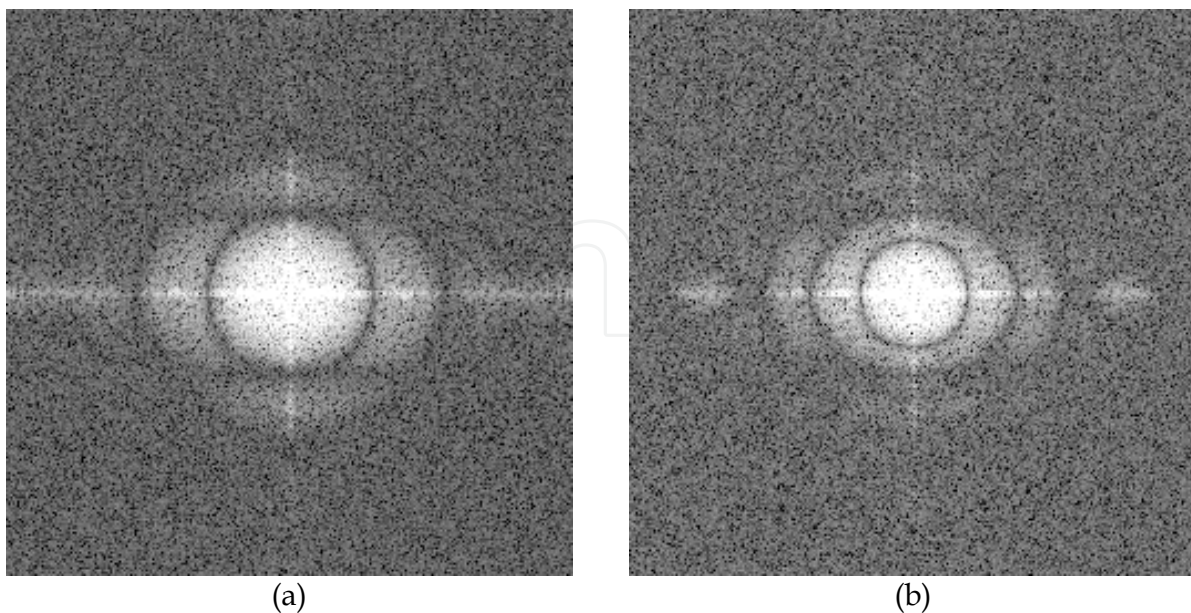
Fig. 6. Spectral magnitudes of the test original image shown in Fig. 4(a) with composite degradations: (a) isotropic defocusing (Eq. 25) with $r = 6$ and 1D motion blur (Eq. 21) with $L = 4$, (b) isotropic defocusing (Eq.25) with $r = 6$ and 1D motion blur (Eq. 21) with $L = 6$.

One can observe that since one of the distortion operators dominates, the spectral magnitudes of composite degradations cannot be synthesized by a simple combination of those of the basic degradation operators. This means that the number of training elements of a matching system should be drastically increased.

In the Fourier representation of images, spectral magnitude and phase tend to play different roles (Oppenheim & Lim, 1981). For instance, in some situations many of the important features of an image are preserved if only the phase is retained. Furthermore, under a variety of conditions, phase information alone is sufficient to completely reconstruct an image to within a scale factor.

(a)   (b)

(c)   (d)
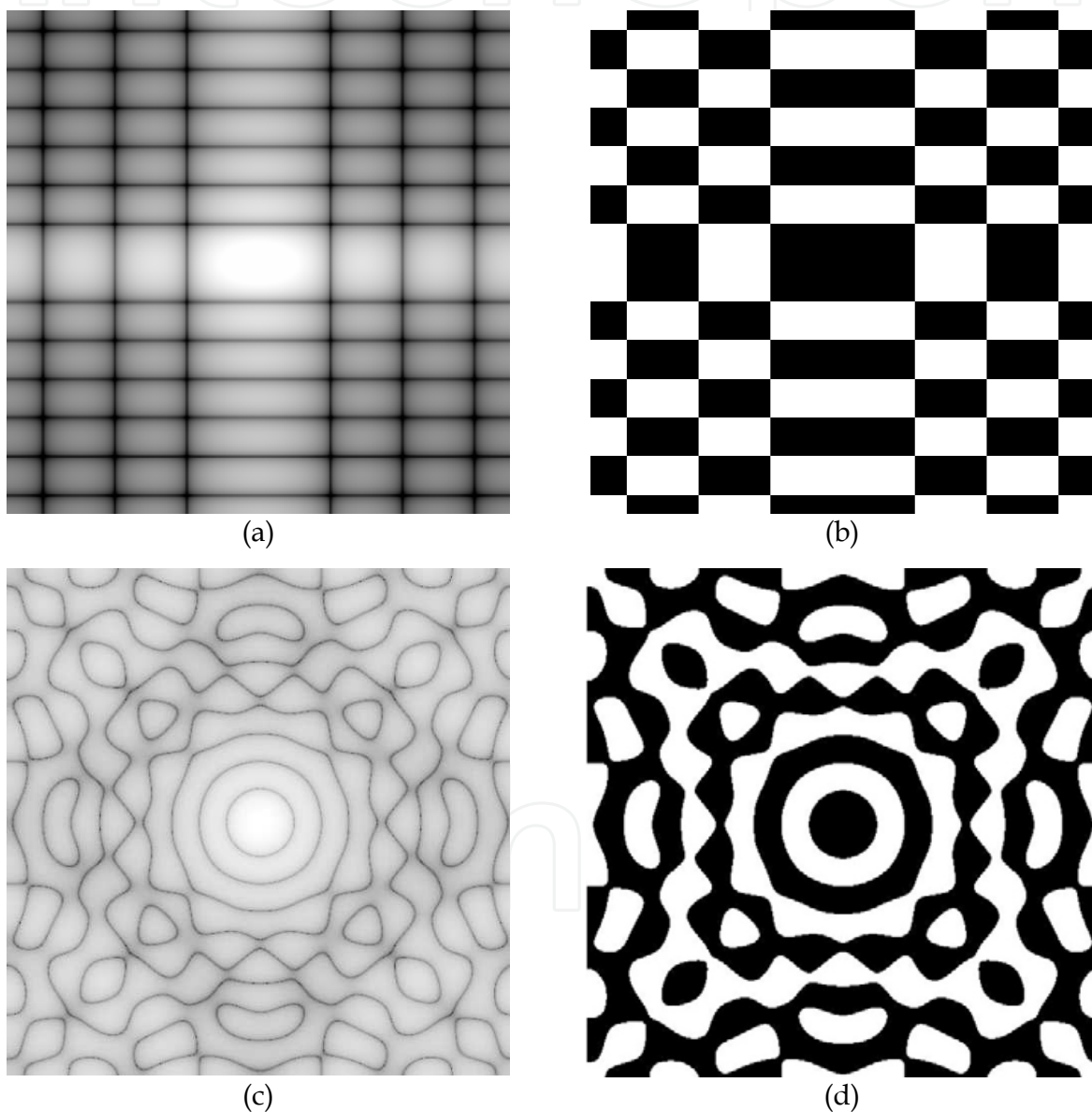
Fig. 7. (a) Cepstrum of the original image degraded by convolution with rectangular aperture (Eq. 27) with a=2, b=4, (b) the difference of phases of the original and distorted (Fig. 7(a)) images, (c) cepstrum of the original image degraded by convolution with circular aperture with radius of 4, and (d) the difference of phases of the original and distorted (Fig. 7(c)) images.

If noise fluctuation in Eq. (19) is small, the phase of the distortion operator is equal to the difference between the phases of the degraded and original images. If the distortion operator is Gaussian, its phase is zero, and the phases of the distorted and original images coincide If the distortion operator is a finite function, e.g. $(x, y) \in W$, then the phase of the distorted image may differ from the phase of the original image by $\pm\pi$, and points at which the phase jumps by $\pm\pi$ coincide with the location of zeros of the spectral magnitude of the degraded image. These zeros, for even functions are all located on the real axis. So, the phase of the original image either coincides with that of the distorted image or differs from that of the distorted image by $\pm\pi$. Fig. 7 shows the differences between the phases of the distorted and original images for rectangular and circular aperture blurs. Therefore, under certain conditions, we can identify the type of the distortion operator and estimate its spectral phase from the observed degraded image.

4. Conclusion

In this chapter we treated the problem of restoring linearly degraded image using two-dimensional image variations. The restored image minimizes the objective functional subject to the Kronrod's variations. In order to achieve a good restoration, it is important take into account topological characteristics of the original image, which are well described by the first Kronrod's variation. The first step in restoring a degraded image is the identification of the type of degradation operator. It can be done by matching of the spectral magnitude of the degraded image with those of created database. Under certain conditions, the phase of the distortion operator may be also estimated from the distorted image. Extensive testing it was shown that the original image can be automatically restored by proper choice of the parameters of the proposed method.

5. Acknowledgment

6. References

Adams, R. A. (1975). *Sobolev Spaces*, Academic Press, ISBN 978-0-12-044150-1, Boston, USA

Banham, M., & Katsaggelos, A. (1997). Digital image restoration. *IEEE Signal Processing Magazine,* Vol. 14, No.2, (March 1997), pp. 24-41, ISSN 1053-5888

Buades, A., Coll, B. & Morel, J.M. (2006). The staircasing effect in neighborhood filters and its solution. *IEEE Trans. Image Process.*, Vol. 15, No. 6, (June 2006), pp 1499-1505, ISSN 1057-7149

Bertero, M. & Boccacci, P. (1998). *Introduction to inverse problems in imaging,* Institute of Physics Publishing, ISBN 0-7503-0435-9, Bristol, UK

Biemond, J., Lagendijk, R.L. & Mersereau, R.M. (1990). Iterative methods for image deblurring. *Proc. IEEE. Vol. 78*, No. 5, (May 1990), pp. 856-883, ISSN 0018-9219

Bovik, A. (2005). *Handbook of image and video processing* (2nd ed.), Academic Press, ISBN 0-12-119792-1, NJ, USA

Cannon, M. (1976). Blind deconvolution of spatially invariant image blurs with phase. *IEEE Trans. Acoust. Speech Sig. Proc.*, Vol. ASSP-24, No. 1, (Fenruary 1976), pp. 58−63 (1976), ISSN: 0096-3518

Chan, T. & Wong, C. (1998). Total variation blind deconvolution. *IEEE Trans. Image Process.*, Vol. 7, No. 3, (March 1998), pp 370–375, ISSN 1057-7149

Gennery, D.B. (1973). Determination of optical transfer function by inspection of frequency-domain plot. *J. Opt. Soc. Am.*, Vol. 63, No. 12, (December 1973), pp. 1571−1577, ISSN 1084-7529

González, R. & Woods, R. (2008). Digital image processing (3rd ed.), Prentice Hall, ISBN 0-13-1687288, NJ, USA

Jain, A.K. (1989). *Fundamentals of digital image processing*, Prentice Hall, ISBN 0-13-332578-4, NY, USA

Kay, S. (1993). *Fundamentals of statistical signal processing: estimation theory*, Prentice Hall, ISBN 0-13-345711-7, NJ, USA

Kundur, D., & Hatzinakos, D. (1996). Blind image deconvolution. *IEEE Signal Processing Magazine,* Vol. 13, No. 3, (May 1996), pp. 73-76, ISSN 1053-5888

Kronrod, A. S. (1950). On functions of two variables. *Uspekhi Mat. Nauk*, Vol. 5, No. 1, (January 1950), pp. 24–134, ISSN 0042-1316

Milukova, O., Kober, V., Karnaukhov, V. & Ovseevich, I.A. (2010). Restoration of blurred images with conditional total variation method. *Pattern Recognition and Image Analysis* Vol. 20, No. 2, (May 2010), pp. 179-184, ISSN 1054-6618

Milukova, O., Kober, V., Karnaukhov, V. & Ovseevich, I.A. (2010). Spectral analysis of distorted images in restoration problems. *Pattern Recognition and Image Analysis* Vol. 20, No. 3, (September 2010), pp. 335-340, ISSN 1054-6618

Milukova, O., Kober, V., Karnaukhov, V. & Ovseevich, I.A. (2011). Iterative global and local methods of image restoration. *Pattern Recognition and Image Analysis* Vol. 21, No. 2, (May 2011), pp. 309-311, ISSN 1054-6618

Oppenheim, A.V. & Lim, J.S. (1981). The importance of phase in signals. *Proceedings of the IEEE*, Vol. 69, No. 5, (May 1981), pp. 529 - 541, ISSN 0018-9219

Perona, P. & Malik, J. (1990). Scale-space and edge detection using anisotropic diffusion. *IEEE Transaction on Pattern Analysis and Machine Intelligence*, Vol. 12, No. 7, (July 1990), pp. 629-639, ISSN 0162-8828

Rudin, L., Osher, S. & Fatemi, E. (1992). Nonlinear total variation based noise removal algorithms. *Phys. D*, Vol. 60, pp. 259–268, ISSN 0167-278

Sezan, M.I. & Tekalp, A.M. (1990). Survey of recent developments in digital image restoration. *Optical Engineering*, Vol. 29, No. 5, (May 1990), pp. 393-404, ISSN 0091-3286

Sroubek, F. & Flusser, J. (2003). Multichannel blind iterative image restoration. *IEEE Trans. Image Process.*, Vol. 12, No. 9, (September 2003), pp. 1094–1106, ISSN 1057-7149

Tikhonov, A.N. & Arsenin, V.Y. (1977). *Solution of ill-posed problems*, Winston & Sons, ISBN 0-470-99124-0, Washington, USA

Vitushkin, A.G. (1955). *On multidimensional variations*, GITTL, Moscow, Russia (in Russian)

Yaroslavsky, L. P. & Eden, M. (1996). *Fundamentals of digital optics*, Birkhauser, ISBN 3-7643-3833-9, Boston, USA
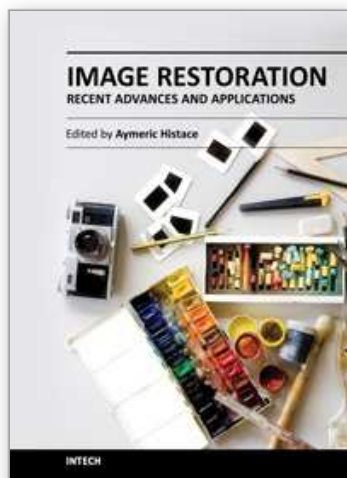
This book represents a sample of recent contributions of researchers all around the world in the field of image restoration. The book consists of 15 chapters organized in three main sections (Theory, Applications, Interdisciplinarity). Topics cover some different aspects of the theory of image restoration, but this book is also an occasion to highlight some new topics of research related to the emergence of some original imaging devices. From this arise some real challenging problems related to image reconstruction/restoration that open the way to some new fundamental scientific questions closely related with the world we interact with.

How to reference

In order to correctly reference this scholarly work, feel free to copy and paste the following:

INTECH
open science | open minds